Mol Neurobiol (2015) 52:562–572
DOI 10.1007/s12035-014-8871-x

Upregulation and Diverse Roles of TRPC3 and TRPC6 in Synaptic Reorganization of the Mossy Fiber Pathway in Temporal Lobe Epilepsy

Chang Zeng · Pinting Zhou · Ting Jiang · Chunyun Yuan · Yan Ma · Li Feng · Renkai Liu · Weiting Tang · Xiaoyan Long · Bo Xiao · Fafa Tian

Received: 19 June 2014 / Accepted: 15 August 2014 / Published online: 12 September 2014

Abstract Temporal lobe epilepsy (TLE) is the most common form of intractable epilepsy and is always accompanied with hippocampal sclerosis. The molecular mechanism of this pathological phenomenon has been extensively explored, yet remains unclear. Previous studies suggest that ion channels, especially calcium channels, might play important roles. Transient receptor potential canonical channel (TRPC) is a novel cation channel dominantly permeable to Ca^{2+} and widely expressed in the human brain. We measured the expression of two subtypes of TRPC channels, TRPC3 and TRPC6, in temporal lobe epileptic foci excised from patients with intractable epilepsy and in hippocampus of mice with pilocarpine-induced status epilepticus (SE), an animal model of TLE. Cortical TRPC3 and TRPC6 protein expressions were significantly higher in TLE patients compared with those in controls. Expression of TRPC3 and TRPC6 protein also increased significantly in the CA3 region of the hippocampus of SE mice. Inhibition of TRPC3 by intracerebroventricular injection of anti-TRPC3 antibody prevented aberrant-sprouted mossy fiber collaterals in the CA3 region, while inhibition of TRPC6 by anti-TRPC6 antibody reduced dendritic arborization and spine density of CA3 pyramidal neurons. Our results indicate that TRPC3 and TRPC6 participate diversely in synaptic reorganization in the mossy fiber pathway in TLE.

Keywords Temporal lobe epilepsy · TRPC3 channel · TRPC6 channel · Synaptic reorganization · Pilocarpine

C. Zeng
Health Management Center, Central South University, Changsha, China

C. Zeng · P. Zhou · L. Feng · W. Tang · X. Long · B. Xiao (✉) · F. Tian (✉)
Department of Neurology, Xiangya Hospital, Central South University, 87 Xiangya Road, Changsha 410008, China
e-mail: xiaobo_xy@126.com
e-mail: tianfafa@gmail.com

T. Jiang
Department of Ultrasonography, Central South University, Changsha, China

C. Yuan
Department of Neurology, Hunan Aerospace Hospital, Changsha, China

Y. Ma
Department of Neurology, The First People's Hospital of Yueyang, Yueyang, China

R. Liu
Department of Neurology, Nanshan Affiliated Hospital of Guangdong Medical College, Shenzhen, China

Introduction

Temporal lobe epilepsy (TLE) is the most common form of intractable epilepsy characterized by spontaneously recurrent seizures, and anteromedial temporal lobectomy with hippocampectomy is needed for patients who become drug-resistant [1]. Until now, the molecular mechanisms underlying the epileptogenesis in TLE remain elusive, but it is widely accepted that hippocampal sclerosis (HS), including neuron loss, astroglial proliferation, mossy fiber sprouting (MFS), and synaptic reorganization, could be a pathological basis for TLE [2].

Previous studies have extensively explored the involvement of ion channels, especially calcium channels, in the development of HS. L-type Ca^{2+} channel blocker nicardipine was demonstrated effective in inhibiting MFS in both in vitro and in vivo models of epilepsy [3]. Another study observed

complete absence of hippocampal neuron loss and MFS, as well as dramatically reduced spontaneous seizures, in Ca(v)3.2(−/−) mice after status epilepticus (SE) [4]. Together, these results indicate calcium channels as critical participants in epileptogenesis. Transient receptor potential canonical channel (TRPC) is a nonselective cation channel dominantly permeable to Ca^{2+}. It consists of seven homologues, TRPC1–TRPC7, based on their sequence similarity [5, 6]. Under physiological conditions, mammalian TRPC channels are widely distributed in a broad spectrum of tissues especially having a strong expression in brain [7–10]. Among the TRPCs, TRPC3 and TRPC6 are the most abundant isoforms in mouse cerebrum [11] and are also rich in the human hippocampus [12]. They have diverse physiological functions in processes including growth cone guidance [13], neurite outgrowth [14], and formation of excitatory synapses [13, 15, 16].

Studies have provided evidence of the correlation between TRPC channels and pathophysiology of many CNS diseases, such as subarachnoid hemorrhage [17], Alzheimer's disease [18], and cerebellar ataxia [19]. Recent attempts have also been made to investigate the involvement of TRPC channels in epileptiform activity or acute pathological changes after SE [20, 21]. However, there has been far less focus on their possible roles in regulating hippocampal plasticity during chronic phase of epilepsy, which is important for revealing the underlying mechanisms of epileptogenesis in TLE. Therefore, the present study selected TRPC3 and TRPC6 as potential candidates in investigating the possible roles of TRPC channels in the HS of TLE. Here, we demonstrated upregulated expressions of TRPC3 and TRPC6 in excised human epileptic cortex and hippocampus of mice with SE. Inhibition of TRPC3 exerted a preventive effect on MFS in the CA3 region. On the other hand, inhibition of TRPC6 caused a significant decrease in dendritic complexity of CA3 pyramidal neurons. These data suggest that TRPC3 and TRPC6 channels may be critical pathogenic factors in the epilepsy-related synaptic remodeling, although their roles may be divergent.

Methods

Patient Evaluation and Tissue Collection

Surgical specimens were obtained from 20 patients (mean age, 26.95±9.383 years; range, 12–52 years) with intractable TLE who had undergone standard cortico-amygdalo-hippocampectomy at Xiangya Hospital, the Second Xiangya Hospital of Central South University, or the Second People's Hospital of Hunan Province. The study was approved by the Ethics Committee of Central South University (Changsha, China), and written informed consents were obtained from the patients or their relatives prior to the surgery. Presurgical assessments included a detailed history, neurological examination, interictal and ictal EEG studies, neuropsychological testing, and neuroradiological studies. All cases showing neoplasm, vascular malformations, posttraumatic, and ischemic lesions on preoperative magnetic resonance imaging (MRI) were excluded. Before surgery, each patient's lesion was localized by high-resolution MRI, 24 h EEG or video-EEG, sphenoidal electrode monitoring, and intraoperative electrocorticography. For comparison, six histologically normal anterior temporal neocortex samples were obtained from patients with head trauma. These subjects (mean age, 30.67± 6.439 years; range, 25–72 years) had no history of epilepsy or exposure to AEDs.

Experimental Animals and Pilocarpine Model Establishment

This study utilized adult C57BL/6 male mice (6–8 weeks of age, 20–27 g) obtained from the Experimental Animal Center, Central South University, Changsha, China. Mice were housed in groups (two to four per cage) under temperature- and humidity-controlled conditions (18–25 °C, 50–60 %, respectively). The housing rooms were maintained on a 12-h light/dark cycle (lights on at 0700 hours) with food pellets and water available ad libitum. Animal procedures were conducted in accordance with our institutional guidelines that comply with the NIH Guide for the Care and Use of Laboratory Animals. SE was induced in experimental animals according to a modified version of Peng's protocol [22]. Briefly, 30 min before pilocarpine administration, mice received intraperitoneal injections (i.p.) of methylscopolamine (1 mg/kg) to reduce peripheral cholinergic effects. Experimental animals were then injected of a single dose of pilocarpine hydrochloride (320–340 mg/kg, i.p.; Sigma, St. Louis, MO, USA) to induce SE. Unlike gradual progression in seizural behavior observed in rats, mice could suddenly develop jumping and wild running and end in tonic seizure without forelimb clonus and rearing. Therefore, the pilocarpine-induced seizures were evaluated according to a modified Racine scale [23]. SE was defined as continuous clonus for 2 h after the onset of category 4 seizures or above. Mice that did not meet this criterion were excluded from this study. Diazepam (5 mg/kg, i.p.; Tianjin Pharmaceutical Industry Jiaozuo Limited Company, Tianjin, China) was administered 2 h after the onset of SE to stop or limit behavioral seizures. Half amount of diazepam was added if the seizures were not stopped 1 h after the first injection. Control animals received identical series of injections, except that pilocarpine was replaced with an equal volume of sterile saline. The reason for using a relatively high dose of pilocarpine was to guarantee an optimal SE rate, although the mortality rate could reach as high as 40 %. To reduce the mortality rate, all mice were placed under a heating lamp and received a daily injection of 0.5–1.0 ml 5 % dextrose in lactate Ringer solution for the first 3 days after SE.

Tissue Processing

Patients

After excision, one part of the temporal cortex was immediately frozen in liquid nitrogen and then stored at −80 °C for the use of Western blot analysis. The other part was immediately fixed in 10 % buffered formalin at 4 °C for 24 h and embedded in paraffin, sectioned at 6 μm for immunohistochemistry.

Animals

At 60 days following SE, animals were perfused transcardially with 30 ml saline followed by 30 ml 4 % paraformaldehyde (PFA) in 0.1 M phosphate buffer (PB, pH 7.4) under 10 % chloral hydrate anesthesia (5 ml/kg i.p.). The brains were removed, postfixed in the same fixative overnight, and rinsed in 0.1 M PB containing 30 % sucrose at 4 °C for 3–5 days. Thereafter, the tissues were frozen and sectioned with a cryostat (Leica, Wetzlar, Germany) at 25 μm.

Immunohistochemistry

Patients

The paraffin-embedded tissue sections were deparaffinized in xylene (100 %), rehydrated in graded ethanol, and incubated in 0.3 % H_2O_2 diluted in methanol for 20 min to quench endogenous peroxidase activity. Antigen retrieval was performed with EDTA (1:50) by heating in a microwave oven. After rinsing with 0.01 M phosphate-buffered saline (PBS) and incubation with 10 % normal goat serum for 2 h at 37 °C to block nonspecific binding, the sections were then incubated with anti-TRPC3 antibody (1:300, rabbit polyclonal antibody, Abcam, Cambridge, UK) or anti-TRPC6 antibody (1:500, rabbit polyclonal antibody, Sigma) at 4 °C overnight, followed by incubation with goat anti-rabbit secondary antibody (Zhongshan Goldenbridge Biotechnology Co., Beijing, China) for 30 min at 37 °C. The immunoreactions were visualized in 3,3′-diaminobenzidine tetrahydrochloride (Zhongshan Goldenbridge Biotechnology Co.). Counterstaining was carried out with hematoxylin. Five randomly chosen visual fields (400×) were imaged on every section using a microscope (BX-50, Olympus, Japan) to count the positive cells.

Animals

The frozen sections were air-dried at room temperature (RT) and incubated in 0.3 % H_2O_2 diluted in methanol for 20 min to quench endogenous peroxidase activity. Antigen retrieval was performed with citrate buffer by heating in a microwave oven. After rinsing with 0.01 M PBS and incubation with 10 % normal goat serum for 2 h at 37 °C to block nonspecific binding, the sections were then incubated with anti-TRPC3 antibody (1:1,000, rabbit polyclonal antibody, Sigma) or anti-TRPC6 antibody (1:150, rabbit polyclonal antibody, Sigma) at 4 °C overnight, followed by incubation with goat anti-rabbit secondary antibody (Zhongshan Goldenbridge Biotechnology Co.) for 30 min at 37 °C. The immunoreactions were visualized in 3,3′-diaminobenzidine tetrahydrochloride (Zhongshan Goldenbridge Biotechnology Co.). The tissue was stained together to avoid background variance. Five sections of each animal were collected. Images from consecutive, nonoverlapping fields (magnification 200×) of CA1, CA3, and hilus area were captured using the BX-50 microscope (Olympus) and High Resolution Pathological Image & Word Analysis System (HPIAS-1000; Wuhan Qianping Image Technology Co., Ltd., Wuhan, China). The gray values of the different layers of each subregion were measured and converted into optical density (OD) values to indicate the expression of protein. The researchers did not know the group information at the time of evaluation.

Western Blot

The frozen epileptic lesions and control samples were dissected on a freezing table and homogenized. Protein was extracted by homogenization in RIPA lysis buffer [50 mM Tris-HCl (pH 7.4), 150 mM NaCl, 1 % NP-40, and 0.1 % sodium dodecyl sulfate (SDS)] mixed with protease inhibitors (1 mM phenylmethanesulfonyl fluoride, PMSF) and centrifuged at 12,000 rpm for 10 min at 4 °C. Protein concentrations were determined using a BCA protein assay kit (Beyotime, Nanjing, China), and the samples were degenerated by being boiled for 5 min diluted in Laemmli buffer. Proteins (50 μg per lane) were then subjected to SDS-PAGE (5 % spacer gel, 60 V; 8 % separation gel, 110 V). The separated proteins were electro-transferred to a polyvinylidene difluoride (PVDF) membrane at 300 mA (TRPC3 for 80 min, TRPC6 for 90 min). Membranes were treated in PBS containing 5 % dried skim milk at RT for 1.5 h to block nonspecific binding. The blots were incubated with primary antibody (TRPC3, 1:500, rabbit polyclonal antibody, Abcam; TRPC6, 1:200, rabbit polyclonal antibody, Sigma; β-actin, 1:800, monoclonal antibody, Boster, Wuhan, China) overnight at 4 °C, followed by 1-h incubation with goat anti-rabbit secondary antibody (Zhongshan Goldenbridge Biotechnology Co.) at RT. The immunoreactive bands were visualized by enhanced chemiluminescence (ECL). Densitometry analyses using Image-Pro Plus software (Media Cybernetics, Silver Spring, MD, USA) were then performed to quantify the immunoblotting. Incubation with anti-β-actin confirmed equivalent protein loading. The ratio of the TRPC3/6 and β-actin band density from the same time was analyzed.

Intracerebroventricular Drug Infusion

SE mice were randomly divided into three groups: anti-C3 group (n=12), anti-C6 group (n=12), and sham (vehicle control) group (n=12). Each group was treated with intracerebroventricular injection of anti-TRPC3 antibody (Sigma, 1:6.5, 2 μl), anti-TRPC6 antibody (Sigma, 2 μl), or PBS (2 μl), respectively at 1 and 15 days following SE, time points when MFS was detectable or stable based on our preliminary results (data not shown). The total volume of cerebrospinal fluid was assumed as 300 μl. The concentration of each antibody was determined by the optimal binding concentration for immunohistochemistry (TRPC3 1:1,000, TRPC6 1:150). Animals were anesthetized with 10 % chloral hydrate (5 ml/kg i.p.) and placed in a stereotaxic frame. Intracerebroventricular (ICV) injections were made directly into the lateral ventricle (1.2 mm lateral and 0.4 mm caudal to the bregma at a depth of 2.5 mm). ICV injection sites were confirmed by dye before perfusion.

Timm Staining

At 60 days following SE, animals were injected with 10 % chloral hydrate and perfused transcardially with 30 ml saline followed by 20 ml of 4 % sodium sulfide solution and 20 ml of 4 % PFA. The brains were removed, postfixed in 4 % PFA overnight, and cryoprotected in 30 % sucrose solution in 0.1 M PB. Cryostat sections of 25 μm thick were cut coronally through the hippocampus and mounted on gelatin-coated slides. The slides were developed in the dark at 26 °C for 45–90 min in a solution of 30 ml of 50 % Arabic gum solution, 10 ml citrate buffer, 15 ml of 5.6 % hydroquinone, and 0.5–1 ml of 17 % $AgNO_3$. After development, the sections were rinsed several times in distilled water, processed for light Nissl staining with cresyl violet, dehydrated, cleared, and coverslipped with Permount. Four sections from the septal area where the two blades of the dentate were equal and formed a V shape were selected for each mouse. Timm staining was assessed in the inner molecular layer (IML) of the dentate gyrus (DG) and the pyramidal and infrapyramidal CA3 regions on each section according to previously proposed Timm scales [24]. Both hippocampi of the specimen were analyzed and the score reflected the mean for the two sides. The average score of the four sections was the Timm score of each mouse. Slides with poor staining or excessive artifact were not scored.

Golgi Staining

For dendritic analysis, Golgi staining was performed at 60 days following SE using the FD Rapid GolgiStain Kit (FD Neurotechnologies, Inc., Ellicott City, MD, USA). Briefly, freshly dissected brains were immersed in solution A and B for 2 weeks at RT and transferred into solution C for 1 week at 4 °C. The brains were sliced using a cryostat (Leica) at a thickness of 100 μm. Dendritic arborization was examined under 20× objectives by quantitating the number of apical dendrite branch (bifurcation) points of CA3 pyramidal neurons. Randomly selected neurons (ten per section) meeting all of the following criteria were analyzed: (1) with typical cell morphology (shown in Fig. 4a), (2) dark and consistent impregnation throughout all dendrites and spines, (3) soma located in the middle third section to minimize the number of truncated branches, and (4) relative isolation from neighboring impregnated cells.

Spine density was determined under 100× oil immersion objectives in selected CA3 pyramidal neurons. Dendritic branches emerging from stratum lucidum (the mossy fiber-recipient layer) were assessed (most were the first- to third-order branches, see Fig. 4a). Three to five segments of branches were randomly chosen for each neuron, while ten neurons were chosen for each brain.

Statistical Analysis

Data were expressed as mean±SEM. Statistical significance was assessed using unpaired Student's t test or one-way ANOVA for multiple group comparisons followed by post hoc Tukey's tests for individual pairwise comparisons. α= 0.05 was the level of test; $p<0.05$ was considered statistically significant. All statistical analyses were two-sided and were performed using Statistical Package for the Social Sciences (SPSS) version 17.0 (SPSS, Chicago, IL, USA).

Results

Expressions of TRPC3 and TRPC6 Proteins Were Increased in the Temporal Cortex of TLE Patients and in the Hippocampus of Mice with Pilocarpine-Induced SE

Both TRPC3 and TRPC6 mRNA were previously detected in the human hippocampus [12]. Here, we first examined the protein levels of TRPC3 and TRPC6 by Western blot in the temporal cortex from TLE patients and normal controls. The bands were respectively detected at levels of 97 kDa (TRPC3) and 106 kDa (TRPC6). Compared with controls, a significant upregulation of TRPC3 and TRPC6 immunoreactivity was observed in the samples from TLE patients ($p<0.01$) (Fig. 1a, c).

Immunohistochemistry further revealed the expression pattern of TRPC3 and TRPC6 proteins. In the control group, TRPC3 and TRPC6 displayed relatively weak staining in the cell bodies and dendrites of neurons in the temporal cortex (Fig. 1b). However, in the TLE group, strong staining for TRPC3 and TRPC6 was observed in the corresponding region

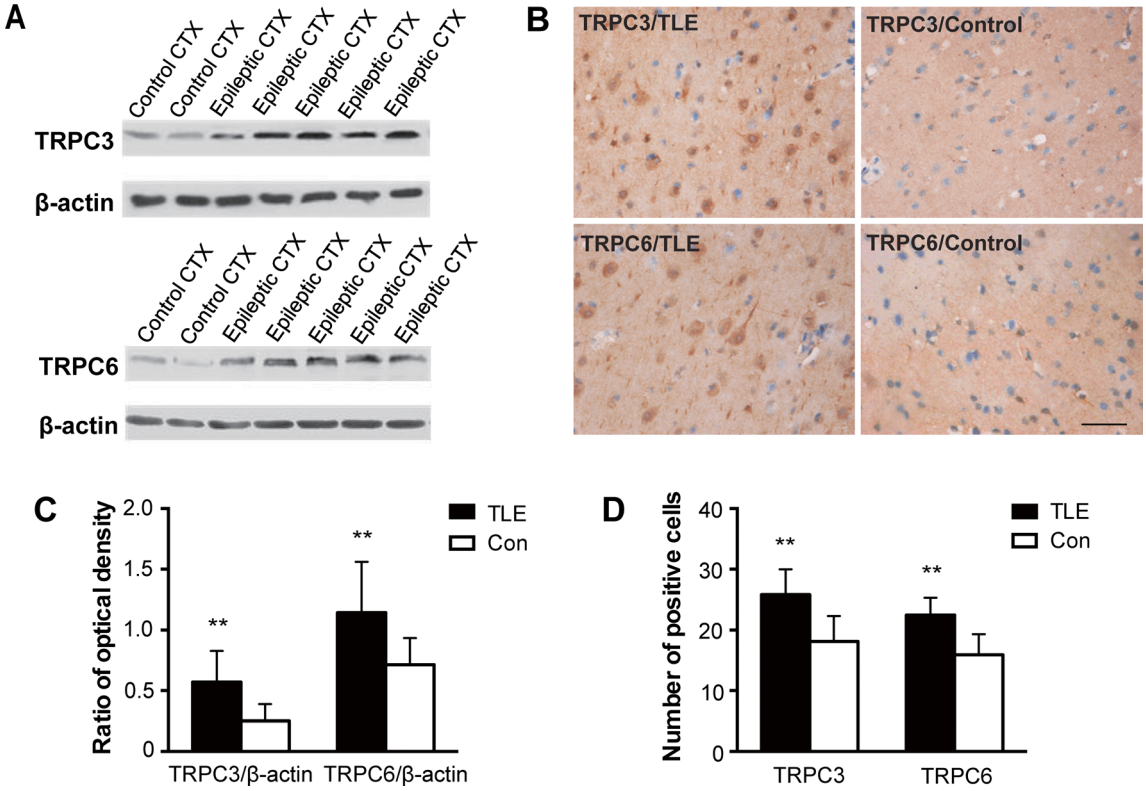

Fig. 1 TRPC3 and TRPC6 protein expression in the temporal cortex of TLE patients and control subjects. **a** Representative Western blot showing TRPC3 and TRPC6 protein expression in the temporal cortex of control subjects and TLE patients. **b** Representative photomicrographs of immunohistochemical staining for TRPC3 and TRPC6 in the temporal neocortex of humans. Strong TRPC3 and TRPC6 immunoreactivity was observed in intractable TLE patients, whereas faint immunoreactivity for TRPC3 and TRPC6 was observed in controls. **c** Densitometric analysis of Western blot. **d** Comparison of positive cells of TRPC3 or TRPC6 between the TLE group (n=20) and control group (n=6). **p<0.01. *Scale bar*=50 μm

(Fig. 1b). Moreover, TRPC3 or TRPC6 positive cells in the temporal cortex from TLE patients significantly increased compared with controls (TRPC3: 25.85±4.13 vs 18.13±4.19, TRPC6: 22.49±2.86 vs 15.93±3.37, p<0.01) (Fig. 1d). Similar results were observed in mouse hippocampus. In the control group, as reported previously in rats [21, 25], TRPC3 immunoreactivity was abundantly detected in the cell bodies and dendrites of CA1-3 pyramidal cells and cell bodies of dentate granule cells (DGCs) and hilar neurons. As previously reported [26], TRPC6 protein was expressed in all the regions of hippocampus, rather than exclusively localized in the molecular layer of the DG as observed by an earlier study [25]. The subcellular expression pattern of TRPC6 protein was similar with TRPC3. Two months after SE, elevated TRPC3 and TRPC6 expressions were observed in the CA3 pyramidal cell layer (Fig. 2e, f), while their expressions in CA1 and DG did not change significantly at the same time point. To better understand the significance of the upregulation of TRPC3 and TRPC6 in the CA3 region, we further performed separate analysis for other layers of CA3. Interestingly, similar expression increases of these two proteins were also seen in the stratum oriens and stratum lucidum of the CA3 region.

Inhibition of TRPC3 Decreased MFS in the CA3 Region Following SE

Many published studies demonstrated CA3 MFS in animals with spontaneous seizures of temporal lobe origin [24, 27, 28]. Interestingly, our current study observed the upregulation of both TRPC3 and TRPC6 exclusively in the CA3 region of hippocampus. This observation led to our postulation that these two TRPC channels might be involved in CA3 MFS. To test our hypothesis, we further investigated the relationship between TRPC3/6 and MFS by performing intracerebroventricular infusion of anti-TRPC3 or anti-TRPC6 antibody in SE mice. In normal controls, stained mossy fibers entered the hilus, and a band of fibers was formed transversing the long axis of the hippocampus, ending in the stratum lucidum, where mossy fibers innervate the apical dendrites of the CA3 pyramidal cells. No obvious Timm granules were seen in the

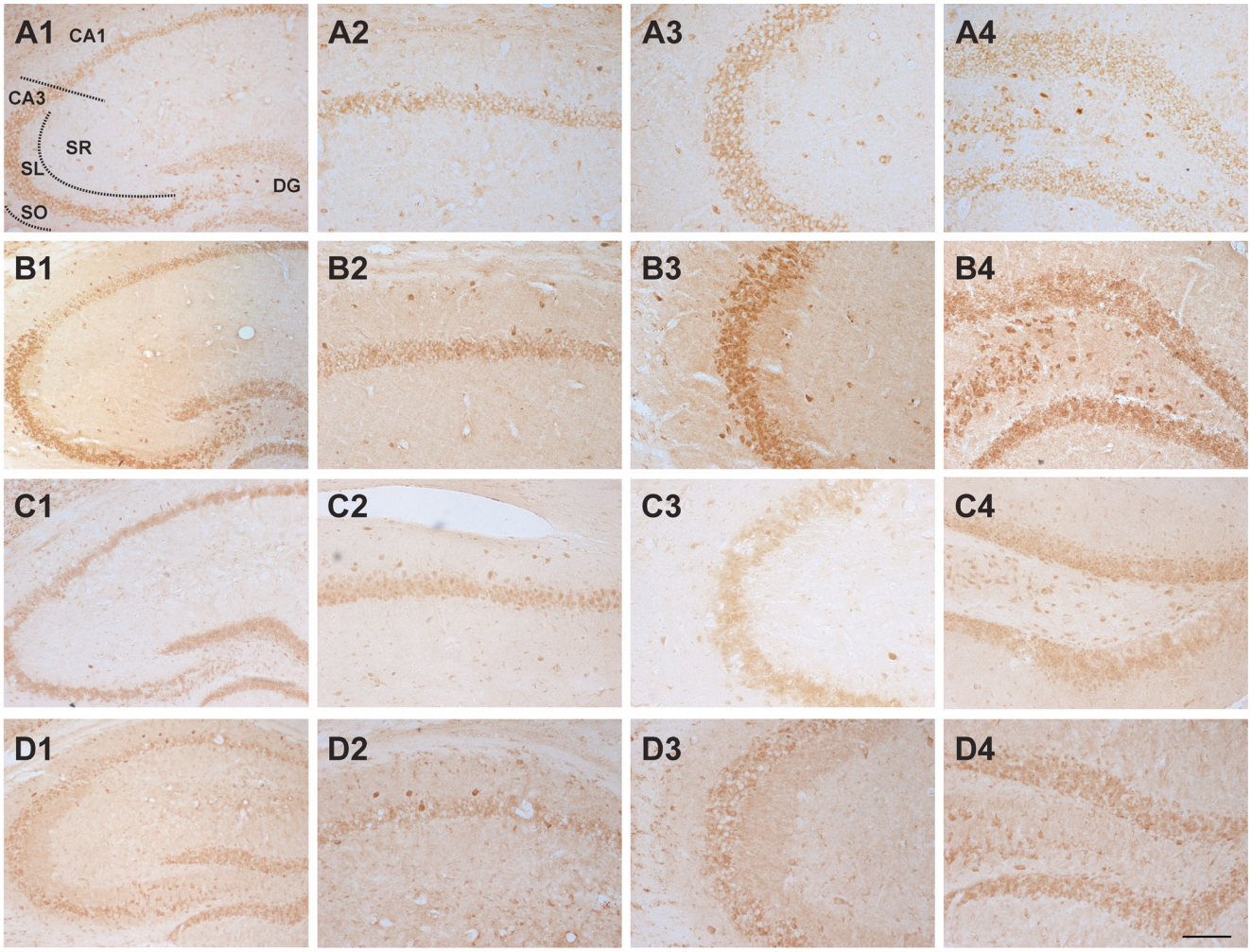

Fig. 2 TRPC3 and TRPC6 expression in the hippocampus of SE mice and controls. Both immunohistochemical staining (**a**–**d**) and quantitative analysis (**e**, **f**) showed increased expressions of TRPC3 and TRPC6 in the pyramidal cell layer, stratum oriens, and stratum lucidum of the CA3 region in SE mice (n=6) compared with that of controls (n=5). *CA1* pyramidal cell layer, *CA3* pyramidal cell layer, *DG* dentate gyrus, *SO* stratum oriens, *SR* stratum radiatum, *SL* stratum lucidum. **p<0.01, *p<0.05. *Scale bar*=200 μm (*A1*, *B1*, *C1*, *D1*) and 100 μm (*A2–A4*, *B2–B4*, *C2–C4*, *D2–D4*)

supragranular region of the dentate gyrus and the pyramidal cell layer and stratum oriens of the CA3 region (Fig. 3a). In the sham group, prominent MFS was observed in the inner molecular layer of the dentate gyrus. In the CA3 region, Timm staining was noted primarily in the pyramidal cell layer, although infrapyramidal staining was also seen (Fig. 3b). Consistently, the Timm scores in the supragranular region and CA3 region of the sham group were significantly higher than those of controls (3.76±0.50 vs

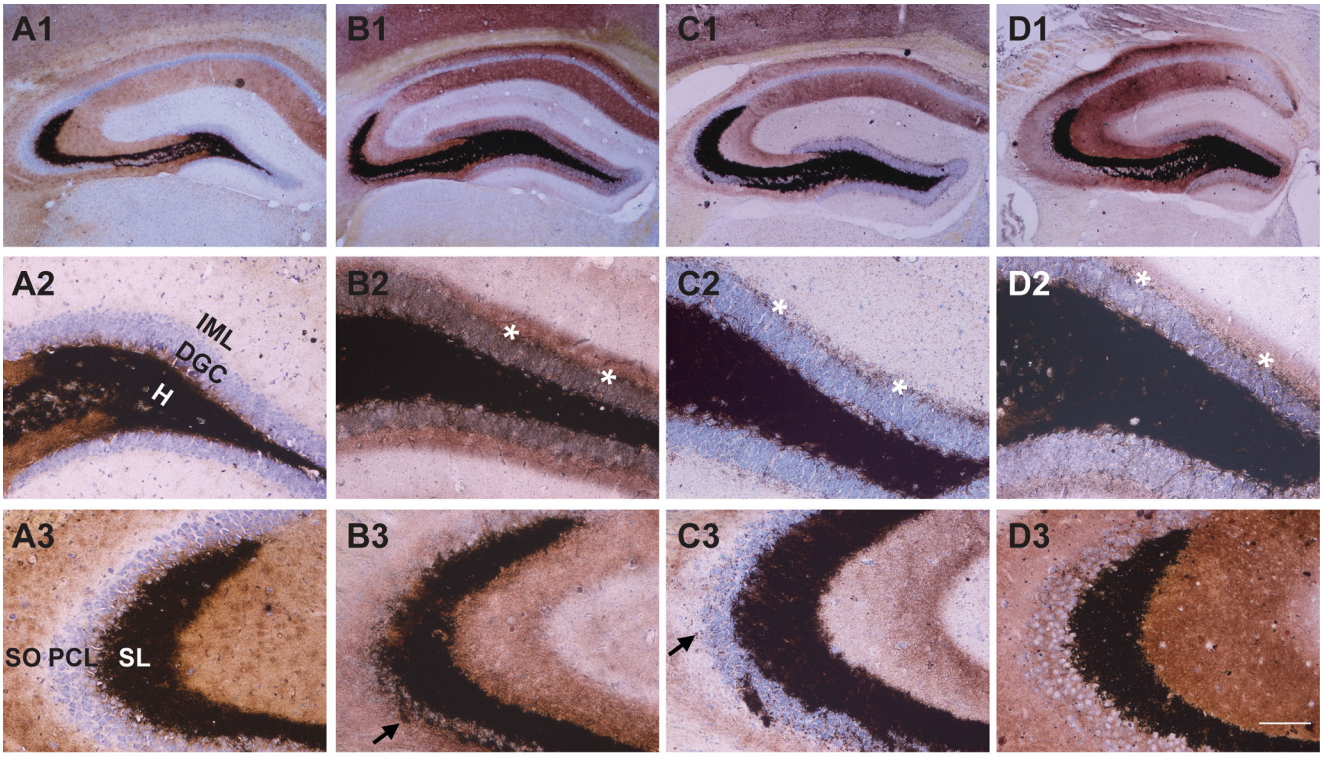

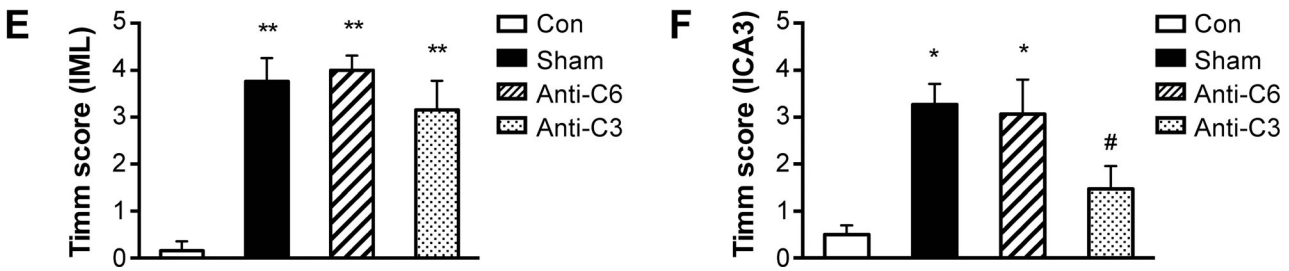

Fig. 3 The effect of anti-TRPC3 and anti-TRPC6 antibodies on MFS in mice hippocampus following SE. No obvious Timm-stained granules were seen in the inner molecular layer of the dentate gyrus and the pyramidal cell layer and stratum oriens in the CA3 region in normal control animals (**a** *A1–A3*). However, Timm staining showed prominent mossy fiber terminals (*asterisk*) in the inner molecular layer in the sham (**b** *B1*, *B2*), anti-C6 (**c** *C1*, *C2*), and anti-C3 (**d** *D1*, *D2*) groups, with Timm scores significantly higher than those of controls (**e**). Timm staining also showed prominent mossy fiber staining (*arrow*) in the pyramidal cell layer and stratum oriens of CA3 in the sham (**b** *B1*, *B3*), anti-C6 (**c** *C1*, *C3*) groups but occasional Timm granules in the pyramidal cell layer in the anti-C3 group (**d** *D1*, *D3*). Note that in the sham group, the pyramidal cell layer narrowed as a result of CA3 pyramidal cell loss (**b** *B3*). The Timm score of the anti-C3 group was significantly reduced compared with that of the sham group and anti-C6 group (**f**). *IML* inner molecular layer, *DGC* dentate granule cell layer, *H* hilus, *SO* stratum oriens, *PCL* pyramidal cell layer, *SL* stratum lucidum. $^{**}p<0.01$, $^{*}p<0.05$, compared with controls; $\#p<0.05$, compared with the sham and anti-C6 groups. *Scale bar*=100 μm

0.15±0.20, $p<0.01$; 3.27±0.45 vs 0.50±0.20, $p<0.05$) (Fig. 3e, f). Treatment with anti-TRPC3 or anti-TRPC6 antibody did not lead to significant changes in Timm score in the supragranular region compared with the sham group (4.00±0.32 and 3.16±0.62 vs 3.27±0.45) (Fig. 3e). However, treatment with anti-TRPC3 antibody significantly reduced Timm score in the CA3 region compared with the sham group (1.47±0.48 vs 3.27±0.45, $p<0.05$) while anti-TRPC6 antibody did not (3.06±0.74 vs 3.27±0.45) (Fig. 3f).

Inhibition of TRPC6 Attenuated Dendritic Remodeling in Area CA3 Following SE

Upregulation of TRPC3 and TRPC6 in the stratum lucidum of CA3, the projection field of granule cell mossy fiber axons and the principal localization of pyramidal cell thorny excrescences, indicates that CA3 pyramidal apical dendrites would be a target of interest. The apical dendrite branch points and spine density of CA3 pyramidal neurons in the sham group

were slightly higher than those in normal controls, but without statistic significance. In anti-C6 group, the apical dendrite branch points and the density of thorns along the second-order dendritic segments of CA3 pyramidal cells were significantly reduced compared to those from the sham group and anti-C3 group ($p<0.05$) (Fig. 4b–d). Similar trends towards reduced thorn density were observed for the third-order dendritic segments, although the effect did not reach significance (Fig. 4c). Treatment of anti-TRPC3 antibody did not produce significant effects on apical dendrite branch points and spine density of CA3 pyramidal neurons compared with the control and sham groups.

Discussion

In our study, we were able to show for the first time the expression levels and patterns of TRPC3 and TRPC6 proteins in the temporal cortex from TLE patients. Both molecular biological and histological measures demonstrated upregulation of each channel protein. Similar observation was obtained in the hippocampus of mice after pilocarpine-induced SE. These findings contrast with a previous report of opposite alterations in TRPC3 and TRPC6 expressions in the hippocampus of rat pilocarpine model [21]. The reasons for the differences are unclear but could be related to the different intervals at which the subjects were studied or to species differences. Such differences, when elucidated, could provide new insights into multiple mechanisms and network alterations involved in TLE.

In the mouse pilocarpine model, we observed an increase in both TRPC3 and TRPC6 expressions specifically in CA3 subfield, a location where aberrant MFS could take place, which suggests that these channels might participate in this axonal reorganization. Indeed, inhibition of TRPC3 prevented MFS in the CA3 region, but not in the IML. This result indicates that TRPC3 may be involved in the generation of epilepsy-associated aberrant projection of the mossy fiber collaterals in the CA3 region. The present study used anti-TRPC3/6 antibodies to suppress TRPC3/6 channel function. Both antibodies have a molecular weight of around 150 kDa. Previous studies by our group and other research groups demonstrated effectiveness of intracerebroventricular delivery of antibodies with similar or even larger size to brain regions including hippocampus [29, 30]. Therefore, it is very likely that anti-TRPC3/6 antibodies have penetrated into the region of interest in our study. However, our results must be interpreted with considerable caution for that we did not directly test the effectiveness of anti-TRPC3/6 antibodies. Future studies are needed to test the functional validity of these antibodies. The possible mechanism of the involvement of TRPC3 channel in MFS could be related to its function in the growth cone guidance and neurite outgrowth. In cultured hippocampal CA1 pyramidal cells, TRPC3 channels are activated by brain-derived neurotrophic factor (BDNF) and implicated in dendritic remodeling [31]. Knockdown of TRPC3 expression with siRNAs inhibits the BDNF-induced turning of growth cones in cultured cerebellar granule cells [13]. Exactly how guidance cues activate TRPC channels on growth cones remains unclear, but it seems that these cues activate phospholipase C [13], which hydrolyses phospholipids into Ins(1,4,5)P3 and diacylglycerol. Ins(1,4,5)P3 activates Ca^{2+} release from the endoplasmic reticulum, and the depletion of these stores can open store-operated Ca^{2+} channels, which include some TRPC channels [32].

Dendritic spines are the main unitary postsynaptic compartments for the excitatory input [33]. Neurons could modulate their capacity for information input by altering the morphology of dendrites like the size and complexity of dendrites and the density, size, and shape of dendrite spines. Recent studies have revealed the important roles of TRPC6 in promoting dendritic growth and spine formation in cultured hippocampal neurons [16, 26]. Consistently, our study found that TRPC6 channel participated in both dendritic spine growth and dendritic arborization in SE mice, indicating that TRPC6 channel acts as an environmental sensor and cellular modulator in epileptic hippocampus. As observed in cultured rat hippocampal neurons, TRPC6 was mainly localized to excitatory postsynaptic sites [16]. This specific subcellular location could facilitate its role in modulating dendritic growth.

Results from previous studies testing the dendritic plasticity of hippocampal neurons after SE are equivocal. A number of studies have observed a significant density decrease or alterations in shape and size of dendritic spines in cortical and hippocampal neurons from SE or chronic epileptic models [34–37]. Conversely, others reported increase of DGC dentritic spines in both TLE patients and rat pilocarpine model [38, 39]. Interestingly, either way of remodeling could be responsible for the hyperexcitability in epilepsy. Increase of dentritic spine density and arborization could increase the postsynaptic area of excitatory synapses, therefore potentiating the transmission efficiency of these synapses. On the other hand, a decrease or loss of dentritic spines could trigger reconstruction of synaptic network, therefore increasing the overall excitability [40]. Differences in observation time and subjects are possible causes for the contradictory results. In the rat pilocarpine model, dendrites of DGCs revealed an extensive spine loss immediately after pilocarpine-induced SE. However, this generalized damage was transient and followed by recovery and plastic changes in spine shape and density, which occurred 15 to 35 days after the initial acute status, i.e.,

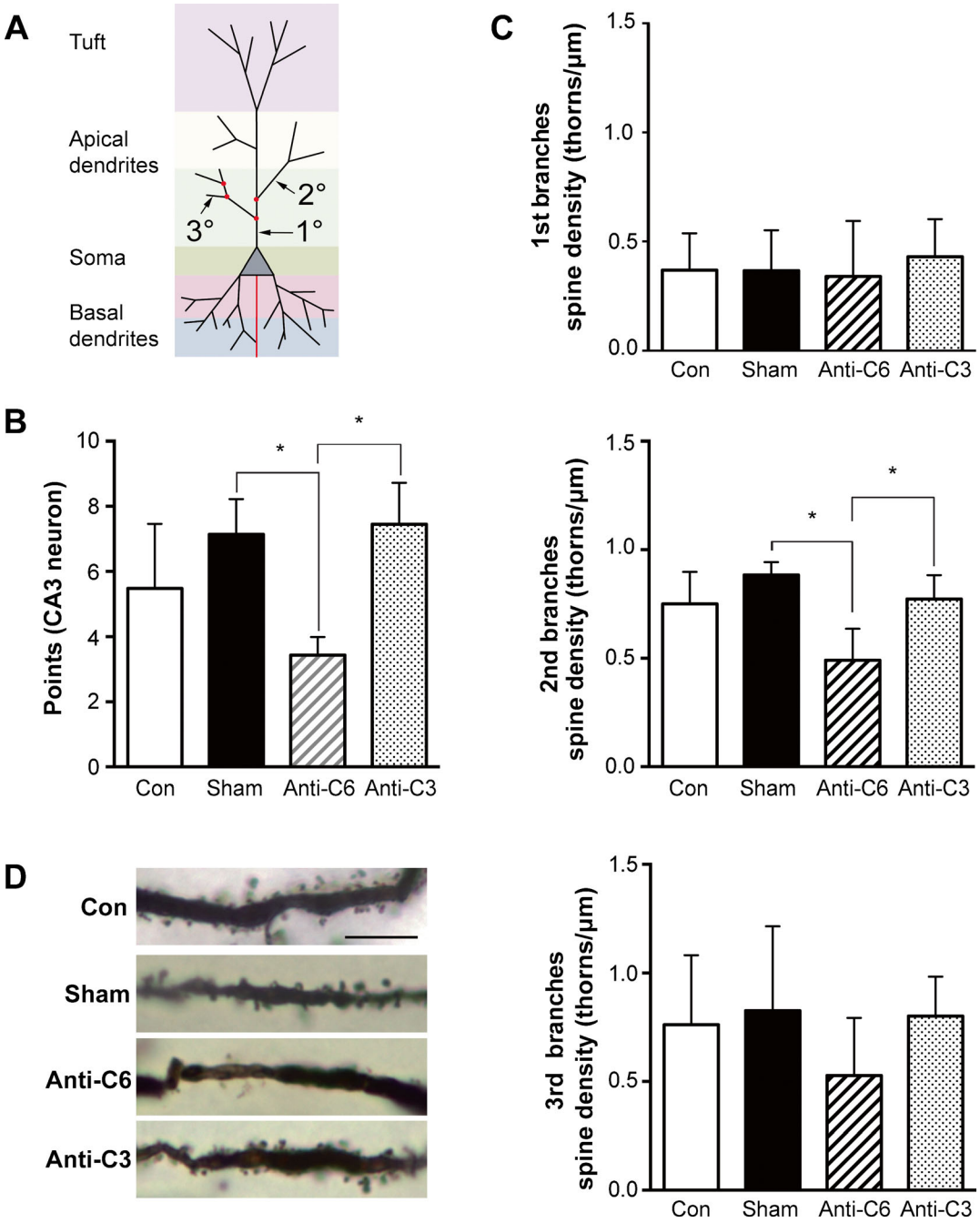

Fig. 4 The effect of anti-TRPC3 and anti-TRPC6 antibodies on dendritic complexity in the CA3 region following SE. **a** A demonstration of a typical CA3 pyramidal neuron. The *red dots* indicate the apical dendrite branch points of CA3 pyramidal neurons; 1°, 2°, and 3° point to the first-, second-, and third-order branches of CA3 pyramidal neurons, respectively. **b** Quantitative analysis of apical dendrite branch points in the stratum lucidum (*the layer with red dots* shown in **a**) of CA3 pyramidal neurons. **c** Quantitative analysis of spine density in dendritic branches with different orders among different groups. **d** Representative images of sections of the second-order dendritic branches and spines in CA3 pyramidal cells from different groups. *Con* control. *$p<0.05$. *Scale bar*=10 μm

the period of establishing a chronic phase of this model with the induction of spontaneous seizures [39]. Another study on TLE patients showed that the number of dendritic branches was significantly lower and spine density was significantly higher in DGCs that had aberrant collaterals. In particular, in the proximal dendrites, the spine density was five times higher in DGCs whose own mossy fibers were sending aberrant collaterals to this dendritic region than the DGCs without such collaterals [41]. Our current study revealed that at 2 months following SE, there was no significant difference in the number of apical dendrite branch points and dendritic spine density of proximal dendrites of CA3 pyramidal neurons

compared with normal controls. However, anti-TRPC6 antibody decreased the number of apical dendrite branch points and dendritic spine density of the second-order dendritic branches of CA3 pyramidal neurons compared with the sham group and anti-C3 group. These results indicate that the dendrites of hippocampal neurons might have experienced a recovery after acute SE-induced injury, and TRPC6 channel could possibly mediate this recovery process.

In conclusion, we report the upregulation of both TRPC3 and TRPC6 channel proteins in the temporal cortex of TLE patients and in the hippocampus of mouse pilocarpine model. Our results also suggest that these two channels participate in different parts of MF axonal remodeling: TRPC3 is involved in the aberrant sprouting of MF in area CA3 while TPRC6 mediates recovery of CA3 pyramidal dendrites after SE-induced damage. These findings open up new possibilities for seeking potential therapeutic targets for TLE.

Acknowledgments The authors sincerely thank the patients and their families for their participation in this study. This work was supported by the National Natural Science Foundation of China (grant no. 81371435). Funding organizations had no influence on the contents or on any other aspect of the article.

Conflict of Interest The authors state no conflict of interest.

References

1. Spencer DD, Spencer SS, Mattson RH, Williamson PD, Novelly RA (1984) Access to the posterior medial temporal lobe structures in the surgical treatment of temporal lobe epilepsy. Neurosurgery 15(5): 667–671
2. Bae EK, Jung KH, Chu K, Lee ST, Kim JH, Park KI, Kim M, Chung CK, Lee SK, Roh JK (2010) Neuropathologic and clinical features of human medial temporal lobe epilepsy. J Clin Neurol 6(2):73–80
3. Ikegaya Y, Nishiyama N, Matsuki N (2000) L-type Ca(2+) channel blocker inhibits mossy fiber sprouting and cognitive deficits following pilocarpine seizures in immature mice. Neuroscience 98(4):647–659
4. Becker AJ, Pitsch J, Sochivko D, Opitz T, Staniek M, Chen CC, Campbell KP, Schoch S, Yaari Y, Beck H (2008) Transcriptional upregulation of Cav3.2 mediates epileptogenesis in the pilocarpine model of epilepsy. J Neurosci 28(49):13341–13353
5. Clapham DE (2003) TRP channels as cellular sensors. Nature 426(6966):517–524
6. Vazquez G, Wedel BJ, Aziz O, Trebak M, Putney JW (2004) The mammalian TRPC cation channels. Biochim Biophys Acta-Mol Cell Res 1742(1–3):21–36
7. Wes PD, Chevesich J, Jeromin A, Rosenberg C, Stetten G, Montell C (1995) TRPC1, a human homolog of a Drosophila store-operated channel. Proc Natl Acad Sci U S A 92(21):9652–9656
8. Zhu X, Chu PB, Peyton M, Birnbaumer L (1995) Molecular cloning of a widely expressed human homologue for the Drosophila trp gene. FEBS Lett 373(3):193–198
9. Harteneck C, Plant TD, Schultz G (2000) From worm to man: three subfamilies of TRP channels. Trends Neurosci 23(4):159–166
10. Montell C, Birnbaumer L, Flockerzi V (2002) The TRP channels, a remarkably functional family. Cell 108(5):595–598
11. Kunert-Keil C, Bisping F, Kruger J, Brinkmeier H (2006) Tissue-specific expression of TRP channel genes in the mouse and its variation in three different mouse strains. BMC Genomics 7:159
12. Riccio A, Medhurst AD, Mattei C, Kelsell RE, Calver AR, Randall AD, Benham CD, Pangalos MN (2002) mRNA distribution analysis of human TRPC family in CNS and peripheral tissues. Mol Brain Res 109(1–2):95–104
13. Li Y, Jia YC, Cui K, Li N, Zheng ZY, Wang YZ, Yuan XB (2005) Essential role of TRPC channels in the guidance of nerve growth cones by brain-derived neurotrophic factor. Nature 434(7035):894–898
14. Greka A, Navarro B, Oancea E, Duggan A, Clapham DE (2003) TRPC5 is a regulator of hippocampal neurite length and growth cone morphology. Nat Neurosci 6(8):837–845
15. Jia YC, Zhou J, Tai YL, Wang YZ (2007) TRPC channels promote cerebellar granule neuron survival. Nat Neurosci 10(5):559–567
16. Zhou J, Du WL, Zhou KC, Tai YL, Yao HL, Jia YC, Ding YQ, Wang YZ (2008) Critical role of TRPC6 channels in the formation of excitatory synapses. Nat Neurosci 11(7):741–743
17. Xie A, Aihara Y, Bouryi VA, Nikitina E, Jahromi BS, Zhang ZD, Takahashi M, Macdonald RL (2007) Novel mechanism of endothelin-1-induced vasospasm after subarachnoid hemorrhage. J Cereb Blood Flow Metab 27(10):1692–1701
18. Yamamoto S, Wajima T, Hara Y, Nishida M, Mori Y (2007) Transient receptor potential channels in Alzheimer's disease. Biochim Biophys Acta-Mol Basis Dis 1772(8):958–967
19. Becker EBE, Olivera PL, Glitsch MD, Banks GT, Achilli F, Hardy A, Nolan PM, Fisher EMC, Davies KE (2009) A point mutation in TRPC3 causes abnormal Purkinje cell development and cerebellar ataxia in moonwalker mice. Proc Natl Acad Sci U S A 106(16):6706–6711
20. Wang M, Bianchi R, Chuang SC, Zhao WF, Wong RKS (2007) Group I metabotropic glutamate receptor-dependent TRPC channel trafficking in hippocampal neurons. J Neurochem 101(2):411–421
21. Kim DS, Ryu HJ, Kim JE, Kang TC (2013) The reverse roles of transient receptor potential canonical channel-3 and -6 in neuronal death following pilocarpine-induced status epilepticus. Cell Mol Neurobiol 33(1):99–109
22. Peng Z, Houser CR (2005) Temporal patterns of fos expression in the dentate gyrus after spontaneous seizures in a mouse model of temporal lobe epilepsy. J Neurosci: Off J Soc Neurosci 25(31):7210–7220
23. Muramatsu R, Ikegaya Y, Matsuki N, Koyama R (2008) Early-life status epilepticus induces ectopic granule cells in adult mice dentate gyrus. Exp Neurol 211(2):503–510
24. Holmes GL, Sarkisian M, Ben-Ari Y, Chevassus-Au-Louis N (1999) Mossy fiber sprouting after recurrent seizures during early development in rats. J Comp Neurol 404(4):537–553
25. Chung YH, Ahn HS, Kim D, Shin DH, Kim SS, Kim KY, Lee WB, Cha CI (2006) Immunohistochemical study on the distribution of TRPC channels in the rat hippocampus. Brain Res 1085:132–137
26. Tai YL, Feng SJ, Ge RL, Du WL, Zhang XX, He ZH, Wang YZ (2008) TRPC6 channels promote dendritic growth via the CaMKIV-CREB pathway. J Cell Sci 121(14):2301–2307
27. Cross DJ, Cavazos JE (2007) Synaptic reorganization in subiculum and CA3 after early-life status epilepticus in the kainic acid rat model. Epilepsy Res 73(2):156–165
28. Tian FF, Zeng C, Guo TH, Chen Y, Chen JM, Ma YF, Fang J, Cai XF, Li FR, Wang XH, Huang WJ, Fu JJ, Dang J (2009) Mossy fiber sprouting, hippocampal damage and spontaneous recurrent seizures in pentylenetetrazole kindling rat model. Acta Neurol Belg 109(4): 298–304
29. Feng L, Long HY, Liu RK, Sun DN, Liu C, Long LL, Li Y, Chen S, Xiao B (2013) A quantum dot probe conjugated with abeta antibody for molecular imaging of Alzheimer's disease in a mouse model. Cell Mol Neurobiol 33(6):759–765

30. Klyubin I, Walsh DM, Lemere CA, Cullen WK, Shankar GM, Betts V, Spooner ET, Jiang L, Anwyl R, Selkoe DJ, Rowan MJ (2005) Amyloid beta protein immunotherapy neutralizes Abeta oligomers that disrupt synaptic plasticity in vivo. Nat Med 11(5):556–561
31. Amaral MD, Pozzo-Miller L (2007) TRPC3 channels are necessary for brain-derived neurotrophic factor to activate a nonselective cationic current and to induce dendritic spine formation. J Neurosci 27(19):5179–5189
32. Minke B, Selinger Z (1996) Role of Drosophila TRP in inositide-mediated Ca2+ entry. Mol Neurobiol 12(2):163–180
33. Hering H, Sheng M (2001) Dendritic spines: structure, dynamics and regulation. Nat Rev Neurosci 2(12):880–888
34. Isokawa M (1998) Remodeling dendritic spines in the rat pilocarpine model of temporal lobe epilepsy. Neurosci Lett 258(2):73–76
35. Ferhat L, Esclapez M, Represa A, Fattoum A, Shirao T, Ben-Ari Y (2003) Increased levels of acidic calponin during dendritic spine plasticity after pilocarpine-induced seizures. Hippocampus 13(7): 845–858
36. Wong M (2005) Modulation of dendritic spines in epilepsy: cellular mechanisms and functional implications. Epilepsy Behav 7(4):569–577
37. Kurz JE, Moore BJ, Henderson SC, Campbell JN, Churn SB (2008) A cellular mechanism for dendritic spine loss in the pilocarpine model of status epilepticus. Epilepsia 49(10):1696–1710
38. Bundman MC, Pico RM, Gall CM (1994) Ultrastructural plasticity of the dentate gyrus granule cells following recurrent limbic seizures: I. Increase in somatic spines. Hippocampus 4(5):601–610
39. Isokawa M (2000) Remodeling dendritic spines of dentate granule cells in temporal lobe epilepsy patients and the rat pilocarpine model. Epilepsia 41(Suppl 6):S14–S17
40. Sierra-Paredes G, Oreiro-Garcia T, Nunez-Rodriguez A, Vazquez-Lopez A, Sierra-Marcuno G (2006) Seizures induced by in vivo latrunculin a and jasplakinolide microperfusion in the rat hippocampus. J Mol Neurosci 28(2):151–160
41. Isokawa M (1997) Preservation of dendrites with the presence of reorganized mossy fiber collaterals in hippocampal dentate granule cells in patients with temporal lobe epilepsy. Brain Res 744(2):339–343